Icarus 264 (2016) 62–71

Contents lists available at ScienceDirect

Icarus

journal homepage: www.journals.elsevier.com/icarus

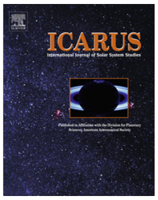

Space weathering trends among carbonaceous asteroids

H.M. Kaluna [a,*], J.R. Masiero [b], K.J. Meech [a]

[a] *Institute for Astronomy, University of Hawaii, 2680 Woodlawn Dr., Honolulu, HI 96822, USA*
[b] *Jet Propulsion Laboratory/Caltech, Pasadena, CA 91109, USA*

ARTICLE INFO

Article history:
Received 4 June 2015
Revised 1 September 2015
Accepted 3 September 2015
Available online 11 September 2015

Keywords:
Spectroscopy
Asteroids, composition
Asteroids, surfaces

ABSTRACT

We present visible spectroscopic and albedo data of the 2.3 Gyr old Themis family and the <10 Myr old Beagle sub-family. The slope and albedo variations between these two families indicate C-complex asteroids become redder and darker in response to space weathering. Our observations of Themis family members confirm previously observed trends where phyllosilicate absorption features are less common among small diameter objects. Similar trends in the albedos of large (>15 km) and small ($\leqslant$15 km) Themis members suggest these phyllosilicate feature and albedo trends result from regolith variations as a function of diameter. Observations of the Beagle asteroids show a small, but notable fraction of members with phyllosilicate features. The presence of phyllosilicates and the dynamical association of the main-belt comet 133P/Elst-Pizarro with the Beagle family imply the Beagle parent body was a heterogeneous mixture of ice and aqueously altered minerals.

1. Introduction

Space weathering studies on asteroids have primarily focused on the alteration of the silicate rich S-complex asteroids. These moderate albedo ($p_v \sim 0.22$; Mainzer et al., 2011) asteroids are known to spectrally darken, redden and have increasingly suppressed absorption bands as a function of time (Belton et al., 1992, 1994; Binzel et al., 1996; Chapman, 1996). These spectral changes are attributed to the vapor deposition of sub-micron metallic iron (SMFe) particles onto grains during micrometeorite impacts and solar wind irradiation (Yamada et al., 1999; Hapke, 2001; Sasaki et al., 2001; Brunetto and Strazzulla, 2005). The intrinsically dark ($p_v \sim 0.06$; Mainzer et al., 2011) nature of carbonaceous material and the lack of prominent absorption features at visible and near-IR wavelengths implied space weathering trends would be difficult to identify for C-complex asteroids (Hapke, 2001; Moroz et al., 1996). However, two recent studies indicate significant spectral slope variation among this class of asteroids as a function of age (Nesvorný et al., 2005; Lazzarin et al., 2006).

Principal component analyses of asteroid colors in the Sloan Digital Sky Survey (SDSS) show the mean slopes of C-complex asteroid families experience a decrease in slopes and become spectrally bluer with age at visible wavelengths (Nesvorný et al., 2005). In contrast, a study using visible spectroscopic data from the Small Main-Belt Asteroid Spectroscopic Survey (SMASSII; Bus and Binzel, 2002b), shows the spectral slopes of the C-complex asteroid population as a whole increase (redden) with age (Lazzarin et al., 2006). However, when Lazzarin et al. (2006) limit their analyses to the C-complex asteroid families they are able to reproduce the slope trends obtained by Nesvorný et al. (2005). Lazzarin et al. (2006) suggest the discrepancies between the two slope trends arise from a sampling effect where the average compositions of C-complex asteroids are not fully represented in the sampled C-complex families.

The Nesvorný et al. (2005) and Lazzarin et al. (2006) studies indicate significant evidence of space weathering trends among the C-complex asteroids, however the effects of compositional variation on these trends is still unclear. In the case of S-complex asteroids, Nesvorný et al. (2005) use the Koronis asteroid family and Karin cluster, which formed from the breakup of a Koronis family member, to study space weathering trends while avoiding the influence of compositional variation. The spectral trends of the young Karin (5 Myr; Nesvorný et al., 2002) and old Koronis asteroids (2.5 Gyr; Marzari et al., 1995) confirm that the reddening observed among the S-complex asteroids is indeed a result of space weathering and not a product of mineralogical variation. The recent discovery of a sub-family of the Themis asteroids allows a similar test to be conducted on C-complex asteroids. The Themis family (Hirayama, 1918) has ~4000 members (Milani et al., 2014) resulting from the catastrophic break up of a 390–450 km parent body asteroid 2.3 Gyr ago (Marzari et al., 1995). A recent

---

* Corresponding author at: Hawaii Institute of Geophysics and Planetology, University of Hawaii, 1680 East-West Road, Pacific Ocean Science & Technology (POST) Building, Honolulu, HI 96822, USA.

E-mail addresses: kaluna@hawaii.edu (H.M. Kaluna), Joseph.Masiero@jpl.nasa.gov (J.R. Masiero), meech@ifa.hawaii.edu (K.J. Meech).

http://dx.doi.org/10.1016/j.icarus.2015.09.007
0019-1035/© 2015 Elsevier Inc. All rights reserved.

(<10 Myr) break up of a Themis family member ($D \sim 20$ km to 65 km in size) resulted in the formation of the Beagle family, which contains ~60 asteroids (Nesvorný et al., 2008). These two families are the first C-complex families identified which originate from the same parent body and provide a unique tool for assessing C-complex space weathering trends while alleviating the mineralogical variations among C-complex asteroids.

In this study we use spectroscopic and albedo data to search for space weathering trends among the Themis and Beagle asteroids. We compare these trends to those of the Veritas asteroid family, which is another young (8.3 Myr; Nesvorný et al., 2003) C-complex family. The Veritas asteroids are not related to the Themis and Beagle asteroids and allow us to assess whether differences in mineralogy affect the spectral trends in space weathering studies of C-complex asteroids.

2. Observations

In this paper, we present data for 52 main-belt asteroids belonging to the Themis, Beagle and Veritas asteroid families. Observations took place on 3.5 nights during March 03, October 29, October 30, 2013 and February 21, 2014 at the 8.2-m Subaru telescope on Maunakea, Hawai'i (see Table 1 for log of observations). Spectroscopic data covering the $0.47 < \lambda < 0.91$ μm spectral range were taken with the Faint Object Camera and Spectrograph (FOCAS). FOCAS has two 2 K × 4 K CCDs with a total of 8 readout channels, each with 512 × 4176 pixels (Kashikawa et al., 2002). The spectra were recorded in channel 3 of chip 2, which has a read noise of 3.4 e- and gain of 2.082 e-/ADU. We used the lowest resolution grating (75 g/mm) and 2 × 2 binning to obtain the highest signal to noise ratio (SNR) for our targets which are dominated by relatively small ($D < 15$ km) and faint asteroids. The resulting low resolution dispersion of 11.8 Å/pixel is ideal for detecting the shallow and broad absorption features typically seen in C-complex asteroid spectra. The SY47 order sorting filter was used to prevent higher order contamination. Observations were taken through a 1.0″ wide slit, oriented to the parallactic angle, while tracking at non-sidereal rates. Due to the lack of non-sidereal guiding and to prevent drifting across the slit, integration times were limited to 600 s.

Family members were selected based on the dynamically derived memberships found in Nesvorný (2012). Previous studies show trends where the frequency of asteroids with absorption features varies as a function of diameter (Florczak et al., 1999; Fornasier et al., 2014), so Themis and Veritas targets were limited to members with similar diameters as Beagle targets ($D \leqslant 15$ km) to avoid size related variations. Nearby solar analog stars were observed at airmasses similar to the asteroids throughout the night and ThAr lamp spectra were taken at the beginning or end of each observing run for wavelength calibration.

3. Data reduction and analysis

Data were reduced using the Image Reduction and Analysis Facility (IRAF) V2.14 `noao` longslit and Subaru `focasred` packages (Tody, 1986). The reduction procedure included overscan and bias subtraction, image trimming, flattening, and cosmic ray removal for long exposure images. The `apall` package was used to perform background subtraction, extraction of the one-dimensional and associated sigma spectra from the two-dimensional images. The sigma spectrum is produced by measuring the sigma at each wavelength in the two-dimensional image. Following extraction, data were wavelength calibrated using emission lines from the ThAr lamp spectra.

Median combined asteroid spectra were divided by nearby G2V solar analog spectra to produce reflectance spectra for each asteroid. The solar analog stars were observed close in time to the observations of each asteroid and were chosen to have an airmass difference of <0.1 to enable extinction correction. The reliability of each solar analog star was tested by producing multiple reflectance spectra of an asteroid from multiple stars at similar airmasses. Only standard stars that produced consistent spectral shapes and slopes were used in producing reflectance spectra. Table 1 reports which solar analog stars were used to produce the reflectance spectra for each asteroid. Residual features due to incomplete removal of sky lines were removed using a median filter to search for erroneous spikes in the final reflectance spectra.

We measured slopes using the equation for the normalized reflectivity gradient S' (reported in units of %/1000 Å), as defined by Jewitt and Meech (1986):

$$S'(\lambda_1, \lambda_2) = \left(\frac{dS/d\lambda}{S_{0.55}}\right) \tag{1}$$

where $dS/d\lambda$ is the slope of the reflectivity measured within the wavelength region between λ_1 and λ_2. Reflectance spectra were normalized to 0.55 μm and spectral slopes were measured using a weighted linear least-squares fit to data between $0.49 < \lambda < 0.91$ μm. The fits were weighted using the IRAF generated sigma spectrum for each asteroid. Data shorter than 0.49 μm were not included in the fit due to potential contamination from the UV absorption below ~0.5 μm created by an Fe^{2+} intervalence charge transfer attributed to phyllosilicates (Vilas, 1994; Hiroi et al., 1996). Asteroid slopes and 1-sigma uncertainties are shown in Table 2.

At large phase angles, asteroids are known to experience an increase in slopes (reddening) (Millis et al., 1976; Bowell and Lumme, 1979; Lumme and Bowell, 1981), however, Luu and Jewitt (1990) find that adopting phase coefficients from other C-complex asteroids does little to improve slope measurements for observations at small phase angles ($\lesssim 40$). In addition, we do not have phase reddening coefficients for most of our targets, but our observations span a small range of phase angles ($\lesssim 20°$), thus no phase reddening correction was applied to our reflectance spectra.

One of the few features found in C-type spectra is a shallow (<5%) 0.7 μm absorption band created by phyllosilicates (Vilas and Gaffey, 1989). To search for this feature we perform continuum removal and fit the 0.55–0.85 μm feature region with a 2nd or 3rd order polynomial. The continuum removed spectra were created by dividing the full spectrum by a linear fit to the 0.7 μm continuum shoulders (0.52–0.54 μm and 0.86–0.88 μm). The continuum removed spectra are shown in Figs. 1–4. The band depth and center were determined using the reflectance value at the wavelength corresponding to the minimum of the polynomial fit. The band depth uncertainty was derived using the uncertainty in the sigma spectrum corresponding to the position of the band center and only features with band depths greater than the associated uncertainties were flagged as a detection. Band depths for objects where features were detected and sensitivity limits computed from the SNR of each spectrum are reported in Table 2.

In addition to our Subaru data, we use visible albedos derived by Masiero et al. (2011) from the Wide-field Infrared Survey Explorer (WISE) to characterize the albedo distributions of Themis, Beagle and Veritas asteroids. We used 2025, 565, and 16 Themis, Veritas and Beagle members, respectively, in our analyses but divided the data set into two size populations (cutoff = 15 km) for consistency with our Subaru data. The mean values for slope and albedo, the standard error of the mean (SEM) and the standard deviations for each family and size range are reported in Table 3. We use the SEM to quantify the variation in our estimate of the mean, and the standard deviation to quantify the dispersion in our slope and albedo distributions.